Physica A 390 (2011) 31–42

Contents lists available at ScienceDirect

Physica A

journal homepage: www.elsevier.com/locate/physa

Interface model for non-equilibrium evaporation

J.P. Caputa *, Henning Struchtrup

Department of Mechanical Engineering, University of Victoria, Canada

ARTICLE INFO

Article history:
Received 12 July 2010
Received in revised form 4 September 2010
Available online 21 September 2010

Keywords:
Liquid–vapor interface
Kinetic theory
Condensation coefficient
Accommodation coefficient
Onsager relations

ABSTRACT

A microscopic interface condition for condensing/evaporating interfaces is developed by combining a velocity dependent condensation probability [T. Tsuruta, H. Tanaka, T. Masuoka, Int. J. Heat Mass Transfer 42 (1999) 4107] and Maxwell type interface conditions with accommodation. Using methods from kinetic theory, macroscopic interface conditions for mass and energy transport across the phase boundary are derived. This model only applies to simple substances, where diffusive effects in the bulk phases are not present. The results are compared to classical non-equilibrium thermodynamics. The interface conditions are considered for the limit of small deviation from equilibrium, and the corresponding Onsager coefficients are computed. These results are useful as boundary conditions for non-equilibrium evaporation and condensation problems, as done previously by our group [M. Bond, H. Struchtrup, Phys. Rev. E 70 (2004) 061605].

1. Introduction

Mass and energy transfer at liquid–vapor phase boundaries are governed by the details of the interaction between vapor molecules and liquid. Molecular dynamics experiments have revealed that faster vapor molecules are more likely to penetrate the liquid where they dissipate their energy to many liquid neighbors and condense, while slower particles are more likely to bounce back into the vapor [1,2]. In the following, a kinetic theory model is presented which accounts for velocity dependent condensation probability. The model describes transport of mass and energy across liquid–vapor phase boundaries in thermal non-equilibrium on the microscopic scale. Macroscopic interface conditions are derived from the model, and the corresponding interface transport coefficients, i.e., the Onsager resistivities, are computed. This model only applies to simple substances, where diffusive effects in the bulk phases are not present.

Most of the classical kinetic theory assumes a constant condensation probability for vapor molecules that hit the liquid surface [3–6]; only a few authors have considered the more general case where the condensation probability depends on the impact velocity [7,8]. The model developed below accounts for the velocity dependence of the condensation probability through the molecular evaporation coefficient θ_c suggested in Ref. [1,2].

The approach is similar to that in Ref. [9], the difference lies in the details of the interface condition. Indeed, the model in Ref. [9] gives asymmetric Onsager coefficients, which can be traced back to the fact that microscopic reciprocity was not taken into account. We consider the model developed below, which includes reciprocity, as a correction. The differences between the new model and the model in Ref. [9] affect the symmetry properties, but not so much the diagonal elements of the resistivity matrix which are dominant for transport characteristics. Thus, the conclusions drawn from the model in Ref. [9] remain valid. The new model can be easily implemented into kinetic theory codes, e.g. DSMC solvers [10], to replace the usual assumption of velocity independent condensation probabilities. The macroscopic interface conditions, on the other hand, serve as boundary conditions for the solution of the equations of classical hydrodynamics, as outlined in detail in Ref. [9].

* Corresponding author.
E-mail addresses: jcaputa@uvic.ca (J.P. Caputa), struchtr@uvic.ca (H. Struchtrup).

0378-4371/$ – see front matter © 2010 Elsevier B.V. All rights reserved.
doi:10.1016/j.physa.2010.09.019

The remainder of the paper is structured as follows. In Section 2 we recall the basic results and definitions of classical Linear Irreversible Thermodynamics (LIT) and apply these to describe the macroscopic interface conditions for evaporation and condensation. Section 3 deals with microscopic kinetic theory interface conditions in general, including the conditions of microreversibility and microscopic reciprocity, which will be used to develop our model in Section 4. The corresponding Onsager coefficients (resistivities) are determined in Section 5. In Section 6 we discuss and re-evaluate the molecular dynamics based determination of Onsager coefficients of Xu et al. [11]; in particular, we show that the data does not suffice to prove Onsager symmetry conclusively. The paper ends with our conclusions.

2. Linear irreversible thermodynamics

Throughout this paper we consider a planar interface between liquid and vapor at which condensation and evaporation occur in 1D steady flows normal to the interface; this scenario is discussed in more detail in Ref. [9]. In the present section we study the macroscopic laws that describe this process.

The balances of energy and entropy at the interface read

$$jh_l + q_l = jh_v + q_v \tag{1}$$

$$\sigma = j(s_v - s_l) + \frac{q_v}{T_v} - \frac{q_l}{T_l} \geq 0, \tag{2}$$

where j is the mass flux across the interface, q_l, q_v are the non-convective energy fluxes in liquid and vapor (as given by Fourier's law), and T_l, T_v, h_l, h_v, s_l, s_v are the respective temperatures, specific enthalpies and entropies at the interface. Moreover, σ is the non-negative entropy generation rate due to evaporation or condensation. For slow evaporation the pressure p of the system is constant [9].

Combining the two equations (1) and (2) by eliminating q_l gives the interfacial entropy production as

$$\sigma = j\left[\frac{g_l}{T_l} - \frac{g_v}{T_v} + h_v\left(\frac{1}{T_v} - \frac{1}{T_l}\right)\right] + q_v\left[\frac{1}{T_v} - \frac{1}{T_l}\right] \geq 0, \tag{3}$$

where $g = h - Ts$ is the Gibbs free energy.

In classical Linear Irreversible Thermodynamics (LIT) [12,13], the entropy production σ is interpreted as a sum of products of thermodynamic fluxes J_α and thermodynamic forces F_α, that is,

$$\sigma = \sum_\alpha J_\alpha F_\alpha, \tag{4}$$

where, in our case,

$$J_\alpha = \{j, q_v\} \tag{5}$$

$$F_\alpha = \left\{\frac{g_l}{T_l} - \frac{g_v}{T_v} + h_v\left(\frac{1}{T_v} - \frac{1}{T_l}\right), \frac{1}{T_v} - \frac{1}{T_l}\right\}. \tag{6}$$

Non-negative entropy production is guaranteed by a linear phenomenological ansatz with a non-negative definite matrix $r_{\alpha\beta}$,

$$F_\alpha = \sum_\beta r_{\alpha\beta} J_\beta. \tag{7}$$

The elements of the matrix $r_{\alpha\beta}$ are the Onsager coefficients, or resistivities.

LIT, as a phenomenological theory, cannot give further insight into the values of the resistivities $r_{\alpha\beta}$, which must either be measured, or be determined from microscopic theories. Most authors expect the matrix to be symmetric [7,8,13,14], $r_{\alpha\beta} = r_{\beta\alpha}$, in extension of the Onsager–Casimir reciprocity relations for transport equations in the bulk, where symmetry results from reversibility of the microscopic laws against velocity reversal [15,16,12,17]. We note that some authors question the general validity of the Onsager–Casimir reciprocity relations, i.e., the symmetry of the Onsager coefficients, as a general rule; rather, they say, their validity must be checked for each individual physical phenomenon [18]. Asymmetric Onsager coefficients were found experimentally in electrical systems in somewhat nonlinear settings [19].

In thermal equilibrium, forces and fluxes vanish so that

$$T_l = T_v = T, \qquad g_l(T, p_{\text{sat}}) = g_v(T, p_{\text{sat}}). \tag{8}$$

These are the well-known conditions of continuous temperature and chemical potential at equilibrium interfaces which define the saturation pressure $p_{\text{sat}}(T)$.

For small deviation from equilibrium the actual pressure, p, will differ only slightly from the saturation pressure of the liquid, $p_{\text{sat}}(T_l)$, and the temperature difference across the interface will be small. Taylor expansion of (6) in $\Delta T = T_v - T_l$ and $\Delta p = p_{\text{sat}}(T_l) - p$ gives, by means of standard thermodynamic property relations, the forces as $F_\alpha = \{\frac{\bar{v}_v - \bar{v}_l}{T_l}\Delta p, -\frac{\Delta T}{T_l^2}\}$,

where $\bar{v}_v$, $\bar{v}_l$ denote the specific volumes at T_l, $p_{\mathrm{sat}}(T_l)$, i.e., at saturation. Since our aim is to compare a model from kinetic theory to the phenomenological laws, we assume pressures well below the critical pressure, for which the vapor can be described by the ideal gas law $pv = RT$ (gas constant R), and the liquid volume can be ignored against the saturated vapor volume (i.e., $\bar{v}_v - \bar{v}_l \simeq \bar{v}_v$). Then, the forces can be further simplified to

$$F_\alpha = \left\{ \frac{R\,\Delta p}{p_{\mathrm{sat}}(T_l)}, -\frac{\Delta T}{T_l^2} \right\}. \tag{9}$$

For convenient comparison to kinetic theory, we introduce dimensionless phenomenological coefficients $\hat{r}_{\alpha\beta}$ by rewriting the phenomenological interface conditions (7) as

$$\begin{bmatrix} \dfrac{\Delta p}{\sqrt{2\pi RT_l}} \\ -\dfrac{p_{\mathrm{sat}}(T_l)}{\sqrt{2\pi RT_l}} \dfrac{\Delta T}{T_l} \end{bmatrix} = \begin{bmatrix} \hat{r}_{11} & \hat{r}_{12} \\ \hat{r}_{21} & \hat{r}_{22} \end{bmatrix} \begin{bmatrix} j \\ \dfrac{q_v}{RT_l} \end{bmatrix}. \tag{10}$$

The matrix $\hat{r}_{\alpha\beta}$ is symmetric if $r_{\alpha\beta}$ is symmetric.

3. Kinetic theory

3.1. Distribution function

In kinetic theory, the behavior of a system of molecules is described by the distribution function $f(x_i, t, c_i)$ which is defined such that $f(x_i, t, c_i)\mathrm{d}\mathbf{c}\mathrm{d}\mathbf{x}$ is the number of molecules with velocities in $\{\mathbf{c}, \mathbf{c} + \mathrm{d}\mathbf{c}\}$ and positions in $\{\mathbf{x}, \mathbf{x} + \mathrm{d}\mathbf{x}\}$ at time t. Given the distribution function, bulk properties such as mass density, momentum density, internal energy, pressure tensor and heat flux can be computed. For comprehensive reviews, see Ref. [20,21].

In the context of evaporating/condensing interfaces, we are interested in the mass flux,

$$j_k = \rho v_k = m \int_{-\infty}^{\infty} c_k f \,\mathrm{d}\mathbf{c}, \tag{11}$$

and the energy flux,

$$Q_k = m \int_{-\infty}^{\infty} \frac{1}{2} c^2 c_k f \,\mathrm{d}\mathbf{c}, \tag{12}$$

where m is the mass of an individual particle, $\rho = \frac{p}{RT}$ is the mass density, and v_k is the vapor velocity.

The distribution function f is a solution of the Boltzmann equation [20,21],

$$\frac{\partial f}{\partial t} + c_i \frac{\partial f}{\partial x_i} = \mathcal{S}(f), \tag{13}$$

where $\mathcal{S}(f)$ denotes the collision term. The balance laws for mass, momentum and energy, as well as the H-theorem (i.e., the second law) can be derived by suitable averaging of the Boltzmann equation over the microscopic velocity [20,21].

In thermal equilibrium, the collision term in (13) must vanish. This implies that the equilibrium distribution is the Maxwellian,

$$f_M(p, T, C) = \frac{p}{mRT} \frac{1}{(2\pi RT)^{3/2}} \exp\left(-\frac{C^2}{2RT} \right). \tag{14}$$

Here, C_k is the peculiar velocity, defined as

$$C_k = c_k - v_k, \tag{15}$$

with the particle velocity c_k and the bulk velocity of the vapor v_k; C denotes the absolute value.

Non-equilibrium solutions of the Boltzmann equation are considerably more complex. The Boltzmann equation can be solved numerically, either directly or by DSMC simulations [10], both of which are computationally expensive; analytical solutions are available only for a few special cases.

The Chapman–Enskog (CE) expansion gives an approximation of the distribution function, which is obtained from (13) by expansion of the distribution function in the Knudsen number Kn. For the evaporation problems considered here, shear stresses can be ignored [9]; then, the first order CE expansion of the Boltzmann equation gives the distribution function [21],

$$f_{\mathrm{CE}} = f_M(p, T, C) \left[1 - \frac{2}{5} \frac{\kappa}{RP} C_k \left(\frac{C^2}{2RT^2} - \frac{5}{2} T \right) \frac{\partial T}{\partial x_k} \right], \tag{16}$$

with the thermal conductivity κ. In particular, the CE distribution gives the energy flux

$$Q_k = \frac{5}{2}RTj_k + q_k \tag{17}$$

where the non-convective heat flux q_k is given by Fourier's law of heat conduction,

$$q_k = -\kappa \frac{\partial T}{\partial x_k}. \tag{18}$$

In Eq. (16), $f_M(p, T, C)$ is a Maxwellian with the vapor bulk velocity v_k. For evaporation problems it is convenient to choose the frame of reference such that the evaporating interface is at rest. For slow evaporation, the vapor velocity is small and the Maxwellian can be approximated as

$$f_M(p, T, C) \backsimeq f_M(p, T, c)\left(1 + \frac{c_k v_k}{RT}\right). \tag{19}$$

Taking only first order terms in vapor velocity and heat flux into account, the distribution (16) reduces to

$$f_{\mathrm{CE}} = f_M(p, T, c)\left\{1 + \frac{c_k v_k}{RT} + \frac{2}{5}\frac{q_k c_k}{pRT}\left(\frac{c^2}{2RT} - \frac{5}{2}\right)\right\}. \tag{20}$$

The distribution (20) will be used for the computation of interface conditions for condensing/evaporating interfaces. This is a simplification of the real conditions, since Knudsen layers [20] in front of the interface are ignored. While this introduces a small error into the analysis, the results are still viable.

3.2. Distribution function at the interface

When a particle from the vapor phase hits the liquid–vapor interface, it interacts with the liquid particles. Depending upon the microscopic conditions for the particular interaction, the particle can be absorbed by the liquid – it condenses – or it might be reflected back into the vapor. The energy of the liquid particles at the interface fluctuates, and occasionally a particle gains enough energy to leave the liquid into the vapor—the particle evaporates.

Evaporation, condensation and reflection processes influence the distribution function at the interface and determine the rates of mass and energy transfer across the interface. We write the distribution function directly at the interface as

$$f_{\mathrm{int}} = \begin{cases} f^-, & c_n' \le 0 \\ f^+, & c_n > 0, \end{cases} \tag{21}$$

where f^- is the distribution of incident particles (negative velocity c_n' normal to the interface), and f^+ is the distribution of emitted particles (positive velocity c_n normal to the interface). The prime at the velocity of incident particles simplifies to distinguish between incident and emitted particles.

The distribution of particles leaving the interface is the sum of a term that describes evaporation, and a term that describes the reflection of non-condensing particles back into the vapor. The relation between the incident and emitted distribution functions can be written as [7,16],

$$f^+ = \theta_e(c_k) f_M(p_{\mathrm{sat}}(T_l), T_l, c) + \frac{1}{|c_n|}\int_{c_n'<0} f^- R_c(c_k' \to c_k)|c_n'|\mathrm{d}\mathbf{c}'. \tag{22}$$

Here, $\theta_e(c_k)$ is the evaporation probability, and $R_c(c_k' \to c_k)$ is the condensation–reflection kernel, both will be discussed shortly.

The liquid side of the interface is assumed to be in local equilibrium [16,22,6,9], and thus evaporating particles leave in a Maxwellian distribution $f_M(p_{\mathrm{sat}}(T_l), T_l, c)$, where T_l is the liquid surface temperature and $p_{\mathrm{sat}}(T_l)$ is the corresponding saturation pressure.

In thermal equilibrium, no net evaporation or condensation occurs, the vapor and the liquid have the same temperatures, $T_v = T_l$, the vapor pressure is equal to the saturation pressure, $p = p_{\mathrm{sat}}(T_l)$, and the vapor is in the corresponding Maxwellian distribution $f_M(p_{\mathrm{sat}}(T_l), T_l, c)$. The latter is ensured by the microreversibility condition [22].

$$f^+|_{\mathrm{eq}} = f^-|_{\mathrm{eq}} = f_M(p_{\mathrm{sat}}(T_l), T_l, c), \tag{23}$$

which is a restriction on evaporation probability and condensation–reflection kernel.

3.3. Condensation–reflection kernel

The condensation–reflection kernel R_c in (22) gives the probability that a particle that hits the interface with velocities in $\{c_k', c_k' + \mathrm{d}c'\}$ will be scattered with velocities in $\{c_k, c_k + \mathrm{d}c\}$ [20].

The reflection probability $\alpha(c_k')$ is the probability that a vapor particle that hits the interface is reflected at all, and the condensation probability $\theta_c(c_k')$ is its complement, thus [7]

$$\alpha(c_k') = 1 - \theta_c(c_k') = \int_{c_n>0} R_c(c_k' \to c_k)\mathrm{d}\mathbf{c} \leq 1. \tag{24}$$

For reflecting interfaces the interaction between particles and interface is described by a reflection kernel $R(c_k' \to c_k)$. Since the probability for an incident particle to leave the reflecting interface is unity, the reflection kernel must satisfy the normalization condition

$$\int_{c_n>0} R(c_k' \to c_k)\mathrm{d}\mathbf{c} = 1. \tag{25}$$

The reflection kernel $R(c_k' \to c_k)$ is subject to the reciprocity relation [16,15,20,7],

$$|c_n'|f_0(T_l, c')R(c_k' \to c_k) = |c_n|f_0(T_l, c)Rt(-c_k \to -c_k'), \tag{26}$$

with the reduced Maxwellian

$$f_0(T_l, c) = \frac{1}{2\pi(RT_l)^2}\exp\left(-\frac{c^2}{2RT_l}\right). \tag{27}$$

For purely reflecting surfaces (i.e., no condensation/evaporation), reciprocity guarantees microreversibility (23).

The proof of the reciprocity condition (26) was first given by Kuscer [15] and later extended by Cercignani [20]. Both proofs are presented for reflecting walls, but not for evaporation and condensation. Nevertheless, it is expected that reciprocity holds also for these processes [16,7], so that the condensation–reflection kernel is reciprocal, that is

$$|c_n'|f_0(T_l, c')R_c(c_k' \to c_k) = |c_n|f_0(T_l, c)R_c(-c_k \to -c_k'). \tag{28}$$

3.4. Evaporation coefficient

The evaporation coefficient θ_e in (22) is determined from the microreversibility condition (23). With the assumption that the liquid phase is in thermal equilibrium [16,22,6], the non-equilibrium in the vapor will not affect the evaporation rate, which therefore can be determined by considering the thermal equilibrium between vapor and liquid.

When the vapor distribution is the equilibrium Maxwellian $f_M(p_{\mathrm{sat}}(T_l), T_l, c')$, the distribution (22) of particles leaving the interface becomes

$$f^+ = \theta_e(c_k)f_{M,sat} + \frac{1}{|c_n|}\int_{c_n'<0} |c_n'|f_{M,sat}'R_c(c_k' \to c_k)\mathrm{d}\mathbf{c}', \tag{29}$$

where we abbreviated $f_M(p_{\mathrm{sat}}(T_l), T_l, c) = f_{M,sat}$ and $f_M(p_{\mathrm{sat}}(T_l), T_l, c') = f_{M,sat}'$.

Substitution of the above into the microreversibility condition (23) gives the evaporation coefficient as

$$\theta_e(c_k) = 1 - \frac{\int_{c_n'<0} |c_n'|f_{M,sat}'R_c(c_k' \to c_k)\mathrm{d}\mathbf{c}'}{|c_n|f_{M,sat}}. \tag{30}$$

Due to the reciprocity of the kernel the evaporation probability equals the condensation probability [7],

$$\theta_e(c_k) = 1 - \int_{c_n'<0} R_c^R(-c_k \to -c_k')\mathrm{d}\mathbf{c}' = \theta_c(-c_k). \tag{31}$$

4. Model for evaporation and condensation

4.1. Maxwell kernel and Tsuruta et al. condensation

The condensation–reflection kernel presented below is based upon combining Maxwell's classical interface condition [20,21] with the condensation probability suggested by Tsuruta et al. [1,2].

The Maxwell kernel, which is frequently used to describe particle–interface interaction in kinetic theory, considers only two simple types of interactions between particles and interface: specular reflection and full thermalization (also known as diffusive reflection) [20,21]. Thermalized particles leave the interface in a Maxwellian distribution governed by the interface temperature T_l.

The Maxwell reflection kernel reads

$$R_M(c_k' \to c_k) = (1-\gamma)\delta(c_k' - c_k + 2n_jc_jn_k) + \gamma|c_n|f_0(T_l, c), \tag{32}$$

where the first term describes specular reflection, and the second term describes thermalization; f_0 is the reduced Maxwellian (27) and n_i is the interface normal. The accommodation coefficient γ is defined as the relative number of thermalizing interactions, $0 \leq \gamma \leq 1$. While the accommodation coefficient could depend on impact velocity, we shall consider it as a constant for simplicity. The Maxwell kernel is properly normalized and fulfills the reciprocity requirement (26).

Based on molecular dynamics simulations for argon-like particles, a velocity dependent condensation coefficient was proposed by Tsuruta and co-workers [1,2],

$$\theta_c(c_n') = \psi \left[1 - \omega \exp\left(-\frac{c_n'^2}{2RT_l} \right) \right]. \tag{33}$$

This condensation probability depends on the normal impact velocity $c_n' = c_k' n_k$. Faster particles are more likely to condense, since they can more easily penetrate the liquid and dissipate their energy to a larger number of neighboring particles. The coefficients ω, ψ are constants that describe the details of the condensation probability. The molecular dynamics simulations indicate that ω and ψ have values in 0.086–0.554 and 0.685–0.971, respectively [1].

4.2. Reciprocal kinetic theory interface model

The Maxwell reflection kernel can be combined with the velocity dependent condensation probability such that the condensation–reflection kernel satisfies the reciprocity requirement (28),

$$R_c(c_k' \to c_k) = \alpha(c_k') \left[(1-\gamma)\delta(c_k' - c_k + 2c_j n_j n_k) + \Lambda \alpha(-c_k)\gamma |c_n| f_0(c) \right]. \tag{34}$$

Here, $\alpha(c_k') = 1 - \theta_c(c_n')$ is the Tsuruta reflection probability (33), and Λ is a normalization coefficient that is obtained as follows:

Inserting the kernel (34) into the definition of the reflection probability (24) gives

$$\alpha(c_k') = \alpha(c_k') \left[(1-\gamma) + \gamma \Lambda \int_{c_{n>0}} |c_n| f_0(c_k) \alpha(-c_k) \mathrm{d}\mathbf{c} \right].$$

Accordingly, the bracket must give unity, which is the case for the normalization coefficient

$$\Lambda = \frac{1}{\int_{c_{n>0}} |c_n| f_0(c) \alpha(-c) \mathrm{d}\mathbf{c}}. \tag{35}$$

4.3. Macroscopic interface fluxes

The next step is to calculate mass and energy fluxes across the interface, and the corresponding transport coefficients. For this, we consider the CE distribution (20) at the interface as the distribution of incoming particles, $f^- = f_{\mathrm{CE}}$. The distribution of emerging particles, f^+, is obtained from (22) by inserting f^- and the Tsuruta–Maxwell kernel (34). We use the resulting distribution function $f = \{f^+, f^-\}$ and the kernel (34) to compute the interfacial mass flux j (11) and the interfacial heat flux Q (12), respectively. After tedious manipulations, the results can be written in the form

$$\begin{bmatrix} j_0 \\ \dfrac{Q_0}{RT_l} \end{bmatrix} = \begin{bmatrix} \mathcal{R}_{11} & \mathcal{R}_{12} \\ \mathcal{R}_{21} & \mathcal{R}_{22} \end{bmatrix} \begin{bmatrix} j \\ \dfrac{Q}{RT_l} \end{bmatrix}, \tag{36}$$

with the forces

$$j_0 = \eta(T_l, T_l) \frac{p_{\mathrm{sat}}(T_l)}{\sqrt{2\pi RT_l}} - \eta(T_l, T_v) \frac{p}{\sqrt{2\pi RT_v}}, \tag{37}$$

$$\frac{Q_0}{RT_l} = 2\varphi(T_l, T_l) \frac{p_{\mathrm{sat}}(T_l)}{\sqrt{2\pi RT_l}} - 2\varphi(T_l, T_v) \frac{p}{\sqrt{2\pi RT_l}} \sqrt{\frac{T_v}{T_l}}. \tag{38}$$

The mean mass and heat transfer coefficients that appear above are defined as

$$\eta(T_l, T) = \psi \left(1 - \frac{T_l \omega}{T_l + T} \right), \tag{39}$$

and

$$\begin{aligned} \varphi(T_l, T) = {} & (1-\gamma)\psi \left(1 - \omega \frac{\left(T_l + \frac{1}{2}T\right) T_l}{(T_l + T)^2} \right) + \gamma \frac{T}{T + T_l} - \gamma [1 - \psi(1-\omega)] \frac{[1 - \psi(1 - \frac{3\omega}{8})]}{1 - \psi(1 - \frac{\omega}{2})} \frac{T_l^2}{T(T + T_l)} \\ & + \gamma \frac{\psi \left[1 - \psi \left(1 - \frac{3\omega}{8} \right) + \frac{\omega}{8} \right]}{1 - \psi \left(1 - \frac{\omega}{2} \right)} \frac{T_l}{T + T_l}. \end{aligned} \tag{40}$$

In thermal equilibrium, where $T_l = T_v$ and $p = p_{\rm sat}(T_l)$, the forces $\{j_0, Q_0\}$ and the fluxes $\{j, Q\}$ vanish. Thus, the model includes the proper equilibrium conditions.

The temperature dependent matrix elements in (36) are

$$\mathcal{R}_{11} = \frac{2-\psi}{2} + \frac{\psi\omega}{2}\frac{T_l^{3/2}\left(T_l + \frac{5}{2}T_v\right)}{(T_l+T_v)^{5/2}}, \tag{41a}$$

$$\mathcal{R}_{12} = -\frac{3\psi\omega}{10}\frac{T_l^{5/2}}{(T_l+T_v)^{5/2}}, \tag{41b}$$

$$\begin{aligned}\mathcal{R}_{21} &= \gamma(1-\psi)\frac{1-\psi\left(1-\frac{3\omega}{8}\right)}{1-\psi(1-\frac{\omega}{2})} + \frac{3}{4}(1-\gamma)\psi\omega\frac{\sqrt{T_l}T_v^3}{(T_l+T_v)^{7/2}} + \frac{21}{8}\psi\omega\frac{T_l^{3/2}T_v^2}{(T_l+T_v)^{7/2}} \\ &\quad + \gamma\psi\omega\frac{1-\psi\left(1-\frac{3\omega}{8}\right)}{1-\psi\left(1-\frac{\omega}{2}\right)}\frac{T_l^{5/2}(T_l+\frac{7}{2}T_v)}{(T_l+T_v)^{7/2}} - \frac{\gamma\psi\omega}{8}\frac{1-\psi(1-3\omega)}{1-\psi(1-\frac{\omega}{2})}\frac{T_l^{3/2}T_v^2}{(T_l+T_v)^{7/2}},\end{aligned} \tag{41c}$$

$$\begin{aligned}\mathcal{R}_{22} &= \left(1-\frac{\gamma}{2}-\frac{\psi}{2}(1-\gamma)\right) - (1-\gamma)\frac{\psi\omega}{10}\frac{T_l^{3/2}T_v^2}{(T_l+T_v)^{7/2}} \\ &\quad + \frac{\psi\omega}{20}\frac{[2(11\gamma-5)(\psi-1)+(5-\frac{19}{2}\gamma)\psi\omega]}{\left[1-\psi\left(1-\frac{\omega}{2}\right)\right]}\frac{T_l^{5/2}}{(T_l+T_v)^{7/2}} \\ &\quad - \frac{7}{40}\psi\omega\frac{\psi\omega\left(1+\frac{2}{7}\gamma\right)-2\left(1+\frac{5}{7}\gamma\right)(1-\psi)}{[1-\psi(1-\frac{\omega}{2})]}\frac{T_l^{5/2}T_v}{(T_l+T_v)^{7/2}}.\end{aligned} \tag{41d}$$

The above expressions for the interface fluxes have the same structure as those presented in Ref. [9]. The details are different, however, since in Ref. [9] a non-reciprocal condensation–reflection kernel was used. Nevertheless, since the structure is the same, the discussion of the relation of the extended model to the classical Hertz–Knudsen [3,4] and Schrage [5] laws remains the same, as long as the new expressions for the coefficients $\eta(T_l, T)$, $\varphi(T_l, T)$ and $\mathcal{R}_{AB}$ are used. For space reasons, we shall not repeat this discussion for the corrected coefficients.

4.4. Linearized fluxes

The kinetic theory based interface relations (36) are nonlinear in the deviations from equilibrium, $\Delta T = T_l - T_v$ and $\Delta p = p_{\rm sat}(T_l) - p$. In order to compare to the dimensionless resistivities $\hat{r}_{\alpha\beta}$ of LIT of Eq. (10), we need to linearize by expanding the equations to first order in the deviations. Expansion of the forces $\{j_0, Q_0\}$ yields

$$\begin{bmatrix} j_0 \\ \dfrac{Q_0}{RT_l} \end{bmatrix} = \mathcal{A}\cdot\begin{bmatrix} \dfrac{\Delta p}{\sqrt{2\pi RT_l}} \\ -\dfrac{p_{\rm sat}(T_l)}{\sqrt{2\pi RT_l}}\dfrac{\Delta T}{T_l} \end{bmatrix}, \tag{42}$$

where the dimensionless matrix $\mathcal{A}$ has the elements

$$\begin{aligned}&\mathcal{A}_{11} = \psi\left(1-\frac{\omega}{2}\right), \qquad \mathcal{A}_{12} = -\frac{\psi}{2}(1-\omega), \qquad \mathcal{A}_{21} = 2\psi\left(1-\frac{3\omega}{8}\right), \\ &\mathcal{A}_{22} = \frac{\psi}{8}(1+\omega) + 2\gamma\frac{1-2\psi\left(1-\frac{7\omega}{16}\right)+\psi^2\left(1-\frac{7}{8}\omega+\frac{5}{32}\omega^2\right)}{1-\psi\left(1-\frac{\omega}{2}\right)}.\end{aligned} \tag{43}$$

To bring the interface conditions (36) into the LIT form (10), we introduce the non-convective heat flux $q_v = Q - jh_v$, where $h_v = \frac{5}{2}RT_v$ is the ideal gas enthalpy of the vapor. Due to linearity, all coefficients must be evaluated at $T_v = T_l$, which gives the dimensionless resistivities as

$$\hat{r} = \mathcal{A}^{-1}\cdot\begin{bmatrix} \left(\hat{\mathcal{R}}_{11}+\dfrac{5}{2}\hat{\mathcal{R}}_{12}\right) & \hat{\mathcal{R}}_{12} \\ \left(\hat{\mathcal{R}}_{21}+\dfrac{5}{2}\hat{\mathcal{R}}_{22}\right) & \hat{\mathcal{R}}_{22} \end{bmatrix}, \tag{44}$$

with the equilibrium values $\hat{\mathcal{R}}_{AB} = \mathcal{R}_{AB}(T_l, T_l)$.

Table 1
The values of the $\hat{r}_{ab}$ matrix coefficients evaluated at the bounding values of the range suggested by Tsuruta et al. for the velocity dependent sticking probability.

γ	ω	ψ	$\hat{r}_{11}$	$\hat{r}_{12}$	$\hat{r}_{21}$	$\hat{r}_{22}$
1	0.086	0.685	1.07	0.115	0.114	0.250
1	0.086	0.971	0.636	0.115	0.115	0.251
1	0.554	0.685	1.47	0.0391	0.0351	0.258
1	0.554	0.971	0.896	0.0427	0.0433	0.270
0.5	0.086	0.685	1.10	0.162	0.162	0.350
0.5	0.086	0.971	0.639	0.123	0.123	0.267
0.5	0.554	0.685	1.49	0.0826	0.0799	0.399
0.5	0.554	0.971	0.901	0.0589	0.0591	0.323
0	0.086	0.685	1.13	0.234	0.235	0.501
0	0.086	0.971	0.643	0.131	0.131	0.284
0	0.554	0.685	1.51	0.163	0.162	0.659
0	0.554	0.971	0.908	0.0796	0.0793	0.390

5. Resistivities

5.1. Impact independent resistivities

In most contributions to classical kinetic theory of phase interfaces it is assumed that the condensation coefficient θ_c does not depend on impact energy, i.e., $\omega = 0$, and that all vapor particles that are not condensing are thermalized, i.e., $\gamma = 1$, so that the constant condensation coefficient ψ is the only parameter. Under these assumptions, accurate kinetic theory calculations give the symmetric matrix of resistivities [6,13,23]

$$\hat{r}_{\text{kin. theory}} = \begin{bmatrix} \dfrac{1}{\psi} - 0.40044 & 0.126 \\ 0.126 & 0.294 \end{bmatrix}. \tag{45}$$

Under the same assumptions, applying the expansion (44) to the model (41), we find

$$\hat{r}_{\omega=0,\gamma=1} = \begin{bmatrix} \dfrac{1}{\psi} - \dfrac{7}{16} & \dfrac{1}{8} \\ \dfrac{1}{8} & \dfrac{1}{4} \end{bmatrix} = \begin{bmatrix} \dfrac{1}{\psi} - 0.437 & 0.125 \\ 0.125 & 0.25 \end{bmatrix}. \tag{46}$$

The exact kinetic theory result accounts for Knudsen layer effects, which were ignored in the derivation of (46). The omission of Knudsen layers explains the – relatively small – differences in the coefficients. Differences in jump and slip boundary conditions due to the omission of Knudsen layer effects are well known in kinetic theory; often one uses correction coefficients to adjust to detailed kinetic theory computations [20].

5.2. Impact dependent resistivities

Fig. 1 shows the values of the resistivity matrix $\hat{r}_{\alpha\beta}$ for pure thermalization, $\gamma = 1$, and Fig. 2 shows the matrix for $\gamma = 0.5$; in both figures the data is plotted over the suggested range for ω and ψ [1]; the actual resistivity values at several choices of values are also included in Table 1. The figures and table show a clear dependence of Onsager resistivities on the parameters ω, ψ, and γ. Depending on the values of these coefficients, the resistivities may differ substantially from their values obtained for velocity independent condensation coefficients as given in (46). Accordingly, it is expected that simulations of non-equilibrium evaporation and condensation processes depend on the values of these coefficients.

Interface models in classical kinetic theory are constructed such that the matrix of Onsager coefficients is symmetric [3–8], and our model follows this lead. Sharipov has proven the symmetry of Onsager coefficients for kernels that obey the reciprocity condition (28) [7,8]. In accordance with this, our model gives symmetric resistivities for all condensation coefficients. While there is no visible asymmetry in the figures, a closer look on the data reveals a very small asymmetry that must be attributed to the omission of Knudsen layers.

6. Onsager coefficients from molecular dynamics simulations

It is extremely difficult to measure the Onsager coefficients for evaporation and condensation, and we are not aware of any experimental measurement that could be used to determine the values of the coefficients $\{\omega, \psi, \gamma\}$.

In an ingenious approach, Xu et al. [13,11] used non-equilibrium Molecular Dynamics (MD) to determine the Onsager coefficients for evaporation and condensation. They determined the Onsager resistivities as defined above in (5)–(7), and for

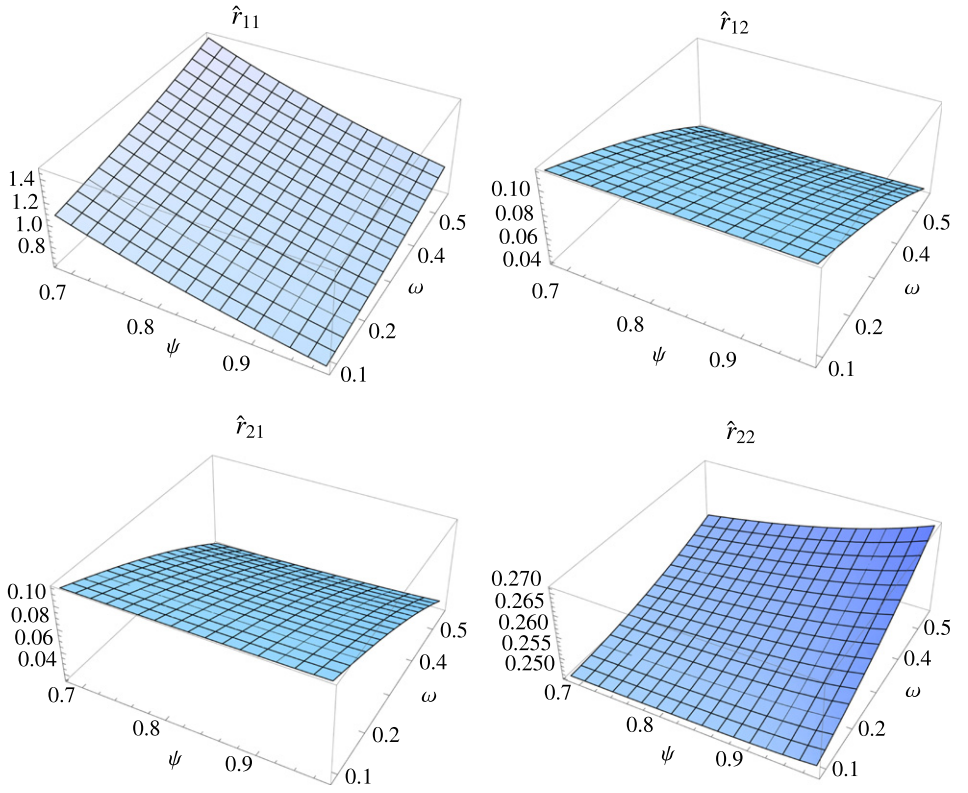

Fig. 1. The matrix elements $\hat{r}_\beta$ plotted for $\gamma = 1$ (pure thermalization) with ψ and ω in the range suggested by Tsuruta et al. [1]; the matrix is symmetric.

an alternative choice of fluxes, where $\{j, q_l\}$ is used instead of $\{j, q_v\}$; we denote the resistivities for this choice as $\bar{r}_{\alpha\beta}$. The off-diagonal coefficients $\bar{r}_{\alpha\beta}$ are related to the resistivities $\hat{r}_{\alpha\beta}$ (10) as $\bar{r}_{\alpha\beta} = \hat{r}_{\alpha\beta} - \Delta\bar{h}\,\hat{r}_{11}$ (for $\alpha \neq \beta$), where $\Delta\bar{h} = (h_v - h_l)/RT_l$ is the dimensionless heat of evaporation.

The results presented in Ref. [11], obtained by using the classical kinetic theory interface prediction for r_{22} and r_{12} of Ref. [6] for determining r_{11} and r_{21}, suggest that the coefficients for the liquid side, i.e., the $\bar{r}_{\alpha\beta}$, are symmetric. However, the data clearly shows strong scatter that does not allow asymmetry to be fully excluded. The results for the vapor side, i.e., the $\hat{r}_{\alpha\beta}$, are subject to even more significant scatter and more clearly do not allow one to exclude asymmetry. Here, it must be noted that $\bar{r}_{12} - \bar{r}_{21} = \hat{r}_{12} - \hat{r}_{21}$, while the absolute values of $\bar{r}_{\alpha\beta}$ are significantly larger than those of $\hat{r}_{\alpha\beta}$; therefore, asymmetry is more difficult to detect for the $\bar{r}_{\alpha\beta}$.

In the MD simulations the vapor is not in the ideal gas regime, and the degree of non-equilibrium is high, so that it is quite difficult to compare to kinetic theory results for ideal gases in the linear regime. Nevertheless, we determine the dimensionless Onsager coefficients from the MD results in Ref. [11]. For this, we rewrite (10) as

$$\begin{bmatrix} \dfrac{p_{\mathrm{sat}}(T_l)}{ZR\sqrt{2\pi RT_l}}F_1 \\ \dfrac{p_{\mathrm{sat}}(T_l)T_l}{Z\sqrt{2\pi RT_l}}F_2 \end{bmatrix} = \begin{bmatrix} \hat{r}_{11} & \hat{r}_{12} \\ \hat{r}_{21} & \hat{r}_{22} \end{bmatrix} \begin{bmatrix} j \\ \dfrac{q_v}{RT_l} \end{bmatrix}, \tag{47}$$

where F_α are the measured thermodynamic forces, j, q_v are the measured fluxes, and $Z = \frac{p_{\mathrm{sat}} v_{\mathrm{sat}}}{RT_l}$ is a real gas correction factor, determined from the Redlich–Kwong equation and the saturation pressure, which are both given in Ref. [11]. Kinetic theory suggests that the dimensionless Onsager coefficients are constants. Then, one can use two pairs (i, j) of the data sets given in Ref. [11] to find the four coefficients $\hat{r}_{\alpha\beta}$ from the four equations

$$\hat{F}_\alpha^{(i)} = \hat{r}_{\alpha\beta}\hat{J}_\beta^{(i)}, \qquad \hat{F}_\alpha^{(j)} = \hat{r}_{\alpha\beta}\hat{J}_\beta^{(j)}. \tag{48}$$

Only 22 of the 48 data sets in Ref. [11] were used: all cases with surface tension below 0.0035 N/m were discarded to ensure sufficient distance from the critical point; cases 7 and 16 were removed since they gave clear outliers, most probably due to nonlinear deviation from equilibrium. The computation was done only for the vapor side with the appropriate data. There are cases with $j \neq 0$ (cases 8,9,10,13,14) and $j = 0$ (cases 27,28,30–32,34,35,38–47); any two cases with $j = 0$ cannot be paired.

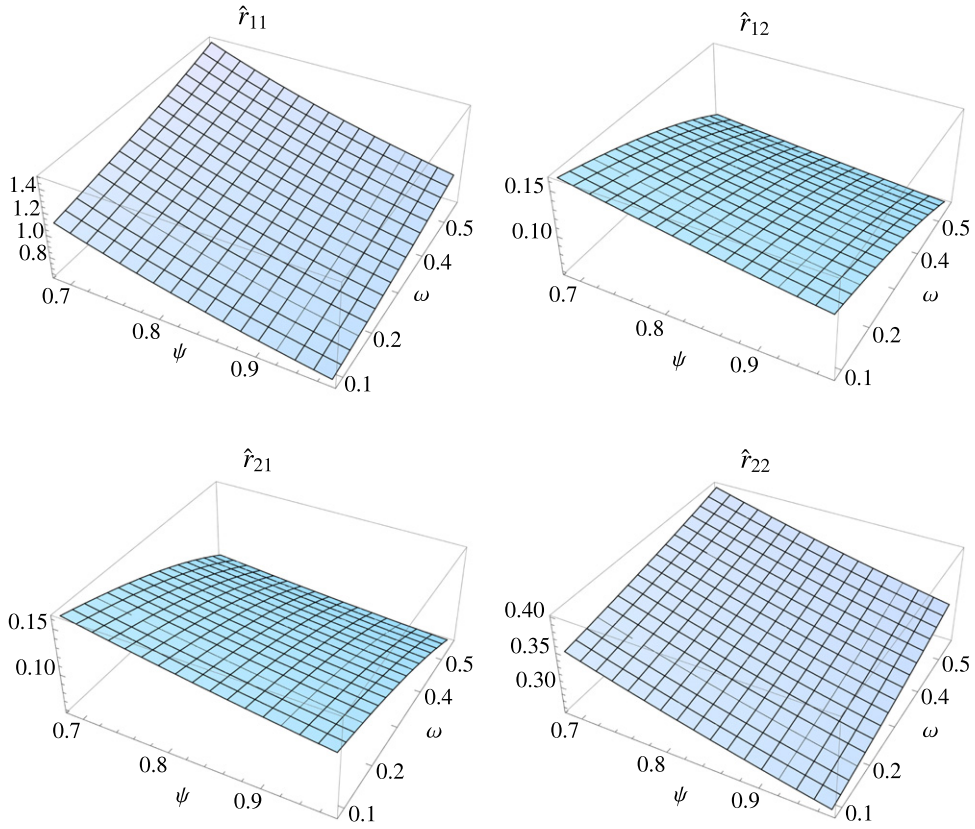

Fig. 2. The matrix elements $\hat{r}_{\alpha\beta}$ plotted for $\gamma = 0.5$ with ψ and ω in the range suggested by Tsuruta et al. [1]; the matrix is symmetric.

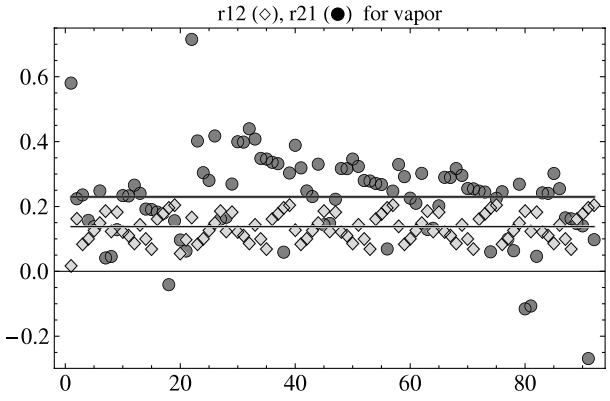

Fig. 3. $\hat{r}_{12}$ (◇) and $\hat{r}_{21}$ (●) for vapor determined from MD data [11]. Due to the large scatter, and the mean values $\langle \hat{r}_{12} \rangle = 0.138$, $\langle \hat{r}_{21} \rangle = 0.229$ might not be meaningful.

Fig. 3 shows the obtained values of the cross coefficients $\hat{r}_{12}$ and $\hat{r}_{21}$ for the 95 different data pairs that were used in the evaluation. There is only a small number of cases with non-zero j, and thus there is not enough data to allow for strong conclusions. In particular, the scatter is relatively large and thus the given mean values might not be meaningful. Nevertheless, asymmetry of the coefficients cannot be excluded. Fig. 4 shows the corresponding values for the diagonal coefficients $\hat{r}_{11}$ and $\hat{r}_{22}$, which also exhibit substantial scatter.

With the scatter observed in the MD data, there is no point in trying to fit the coefficients $\{\omega, \psi, \gamma\}$ to the MD simulations. Indeed, in the MD simulations the temperatures of liquid and vapor differ by more than 10%, which makes it likely that the MD experiments are in the nonlinear regime, for which symmetry cannot be expected. Moreover, real gas effects play a role, and it is unclear how to properly correct the MD data for these. Without more accurate data, a proper fit for the coefficients is not possible.

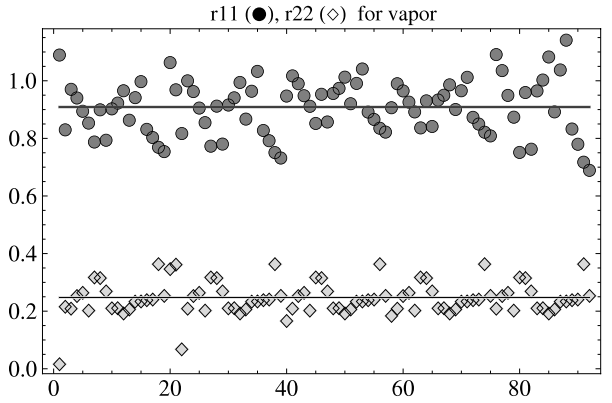

Fig. 4. $\hat{r}_{11}$ (•) and $\hat{r}_{22}$ (◇) for vapor determined from MD data [11]. Due to the large scatter, the mean values $\langle\hat{r}_{11}\rangle = 0.909$, $\langle\hat{r}_{22}\rangle = 0.248$ might not be meaningful.

7. Summary

In this paper we constructed a microscopic interface condition for evaporating and condensing phase interfaces, based on a velocity dependent condensation probability and Maxwell's reflection model. Macroscopic interface conditions were derived from the microscopic model.

We are not aware of other attempts in the literature to construct a detailed evaporation–reflection kernel with velocity dependent condensation that can be used in kinetic theory. Therefore, the model presented here, and its precursor in Ref. [9], must be seen as a first attempt to link velocity dependent condensation probability with macroscopic equations at the phase interface.

We emphasize that transport is governed by all terms of the Onsager matrix. As can be seen in Figs. 1 and 2, the resistivity matrices depend markedly on the coefficients $\{\omega, \psi, \gamma\}$ in the condensation probability, which therefore affect the macroscopic behavior at phase boundaries.

Molecular dynamics simulations of phase interfaces do not allow us to conclude on Onsager symmetry, most likely due to real gas effects and nonlinearity. The kinetic theory interface model (34) and its macroscopic counterpart (36) can be used to study nonlinear effects at evaporating/condensing interfaces in more detail.

Indeed, reliable macroscopic models that include as much of the microscopic behavior as possible should be highly useful for increased understanding of non-equilibrium condensation and evaporation.

Recently, Phillips and co-workers measured the Onsager coefficients of heat transport across stationary liquid/vapor interfaces in pure substances (reviewed in Ref. [24]). We are currently comparing our kinetic theory model to these measurements; this shall be a subject of a future paper.

Acknowledgements

HS gratefully acknowledges helpful discussions with D. Bedeaux and S. Kjelstrup (Trondheim). This research was supported by the Canadian Space Agency (CSA) and the Natural Sciences and Engineering Research Council (NSERC).

References

[1] T. Tsuruta, H. Tanaka, T. Masuoka, Int. J. Heat Mass Transfer 42 (1999) 4107.
[2] G. Nagayama, T. Tsuruta, J. Chem. Phys. 118 (2003) 1392.
[3] H. Hertz, Ann. Phys. Chem. 17 (1882) 177.
[4] M. Knudsen, Ann. Phys. Chem. 47 (1915) 697.
[5] R.W. Schrage, A Theoretical Study of Interphase Mass Transfer, Columbia University Press, New York, 1953.
[6] J.W. Cipolla, H. Lang, S.K. Loyalka, J. Chem. Phys. 61 (1974) 69.
[7] F. Sharipov, Physica A 203 (1994) 437–456.
[8] F. Sharipov, Physica A 203 (1994) 457–485.
[9] M. Bond, H. Struchtrup, Phys. Rev. E 70 (2004) 061605.
[10] G.A. Bird, Molecular Gas Dynamics and the Simulation of Gas Flows, Clarendon Press, Oxford, 1994.
[11] J. Xu, S. Kjelstrup, D. Bedeaux, A. Røsjorde, L. Rekvig, J. Colloid Interface Sci. 299 (2006) 452.
[12] S.R. de Groot, P. Mazur, Non-Equilibrium Thermodynamics, Dover, New York, 1984.
[13] S. Kjelstrup, D. Bedeaux, Non-Equilibrium Thermodynamics of Heterogeneous Systems, World Scientific, 2008.
[14] V.I. Roldughin, V.M. Zhdanov, Adv. Colloid Interface Sci. 98 (2002) 121.
[15] I. Kuscer, Surf. Sci. 25 (1971) 225.
[16] I. Kuscer, J. Phys. A: Math. Gen. 13 (1980) 621.
[17] H.C. Öttinger, Beyond Equilibrium Thermodynamics, Wiley, Hoboken, 2005.
[18] I. Müller, A History of Thermodynamics—The Doctrine of Energy and Entropy, Springer, Berlin, 2007.

[19] G. Kriza, A. Jánossy, L. Forró, Phys. Rev. B 41 (1990) 5451–5454.
[20] C. Cercignani, Theory and Application of the Boltzmann Equation, Scottish Academic Press, Edinburgh, 1975.
[21] H. Struchtrup, Macroscopic Transport Equations for Rerefied Gas Flows, Springer, Berlin, 2005.
[22] K.W. Kolasinski, Surface Science, Wiley, Hoboken, 2008.
[23] D. Bedeaux, L.J.F. Hermans, T. Ytrehus, Physica A 169 (1990) 263.
[24] L.F. Phillips, Chem. Phys. Lett. 495 (2010) 1–7.